Z-99 WAVE-EQUATION ANGLE-DOMAIN IMAGING FOR MULTICOMPONENT SEISMIC DATA

P. SAVA AND S. FOMEL*
Bureau of Economic Geology, The University of Texas at Austin, Austin, TX 78758, USA

1 Summary

Seismic images obtained by multicomponent wave-equation migration can be decomposed into angle-gathers with a transformation that generalizes the equivalent construction for primary waves. A particularly simple formulation is to use all three components of the offset vector separating sources and receivers at image points. Using full vector offsets, multicomponent angle-gathers are built using simple transformations that are implemented partially in the Fourier domain and partially in the space domain.

2 Introduction

Downward wave extrapolation provides an accurate method for seismic imaging in structurally complex areas (Gray et al., 2001). In order to gain access to velocity and amplitude information, several authors (de Bruin et al., 1990; Rickett and Sava, 2002; Sava and Fomel, 2003; Biondi and Symes, 2004) suggested methods for constructing angle gathers from downward-continued wavefields. The key element for imaging in the angle domain is the imaging condition, that must fulfill two requirements: it must preserve the velocity information during imaging, and it must allow angle decomposition after imaging.

Multicomponent imaging with converted waves gains increasing popularity, since converted waves sample complex geology differently from primary waves and provides different complementary information (Stewart et al., 2002, 2003). In particular, imaging multicomponent data in the angle domain leads to amplitude information (AVA) that can be accurately exploited by rock physics for rock and fluid properties that are different from those inferred from P waves. This paper derives the angle decomposition for converted waves as a generalization of the analogous method for P waves.

3 Imaging condition for shot-record migration

A prestack imaging condition for wavefield extrapolation migration estimates reflectivity at every image point using the following expression (Sava and Fomel, 2005):

$$\mathbf{R}(\mathbf{m},\mathbf{h}) = \sum_{\omega} \mathbf{U}_s(\mathbf{m}-\mathbf{h},\omega)\,\overline{\mathbf{U}_r}(\mathbf{m}+\mathbf{h},\omega)\ . \tag{1}$$

Here, $\mathbf{m} = \left[m_x, m_y, m_z\right]$ is a vector describing the locations of image points, $\mathbf{h} = \left[h_x, h_y, h_z\right]$ is a vector describing the local source-receiver separation in the image space. m_x and m_y are the horizontal coordinates, and m_z is the depth coordinate of an image point relative to a reference coordinate system. The components of the $\mathbf{h}$ vector are the two conventional horizontal offsets, h_x and h_y (Rickett and Sava, 2002), and a vertical offset h_z (Biondi and Symes, 2004). The summation over temporal frequencies ω extracts the image $\mathbf{R}$ at zero time. $\mathbf{U}_s$ and $\mathbf{U}_r$ are the source and receiver wavefields

extrapolated with slownesses s_s and s_r. For P-S reflections, the two slownesses can be written function of the P wave slowness $s(\mathbf{m})$ and the v_p/v_s ratio $\gamma(\mathbf{m})$ at every location in space: $s_s = s$ and $s_r = \gamma s$.

Reflectivity versus angle (RVA) analysis for converted waves requires image decomposition function of angles at every image point $\mathbf{R}(\mathbf{m},\mathbf{h}) \Longrightarrow \mathbf{R}(\mathbf{m},\theta_s,\theta_r)$, where θ_s is the angle made by the incident (source) ray with the normal to the reflector, and θ_r is the angle made by the reflected (receiver) ray with the normal to the reflector (Figure 1).

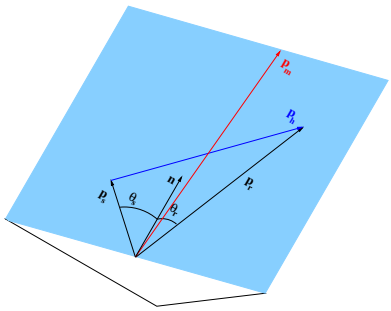

Figure 1: Geometric relations between ray vectors at a reflection point.

4 Angle decomposition

Using the definitions introduced in the preceding section, we can make the standard notations for the source and receiver coordinates: $\mathbf{s} = \mathbf{m} - \mathbf{h}, \mathbf{r} = \mathbf{m} + \mathbf{h}$. The traveltime from a source to a receiver is a function of all spatial coordinates of the seismic experiment $t = t(\mathbf{m},\mathbf{h})$. Differentiating t with respect to all components of the vectors $\mathbf{m}$ and $\mathbf{h}$, and making the standard notations $\mathbf{p}_\alpha = \nabla_\alpha t$, where $\alpha = \{\mathbf{m},\mathbf{h},\mathbf{s},\mathbf{r}\}$, we can write:

$$\mathbf{p_m} = \mathbf{p_r} + \mathbf{p_s}\,, \tag{2}$$

$$\mathbf{p_h} = \mathbf{p_r} - \mathbf{p_s}\,. \tag{3}$$

By definition, $|\mathbf{p_s}| = s_s$ and $|\mathbf{p_r}| = s_r$, where s_s and s_r are slownesses associated with the source and receiver rays, respectively.

For computational reasons, it is convenient to define the angles θ and δ using the following relations: $2\theta = \theta_s + \theta_r$, $2\delta = \theta_s - \theta_r$. Angle 2θ represents the opening between and incident and a reflected ray, and angle δ represents the deviation of the bisector of the angle 2θ from the normal to the reflector. For P-P reflections, $\delta = 0$.

4.1 Reflection angle θ

By analyzing the geometric relations of various $\mathbf{p}_\alpha$ vectors (Figure 1), we can write the following trigonometric expressions:

$$|\mathbf{p_h}|^2 = |\mathbf{p_s}|^2 + |\mathbf{p_r}|^2 - 2|\mathbf{p_s}||\mathbf{p_r}|\cos(2\theta)\,, \tag{4}$$

$$|\mathbf{p_m}|^2 = |\mathbf{p_s}|^2 + |\mathbf{p_r}|^2 + 2|\mathbf{p_s}||\mathbf{p_r}|\cos(2\theta)\,, \tag{5}$$

$$\mathbf{p_m}\cdot\mathbf{p_h} = |\mathbf{p_r}|^2 - |\mathbf{p_s}|^2\,. \tag{6}$$

We can transform this expression further using the notations $|\mathbf{p_s}| = s$ and $|\mathbf{p_r}| = \gamma s$, where $\gamma(\mathbf{m})$ is the v_p/v_s ratio, and $s(\mathbf{m})$ is the slowness associated with the incoming ray at every image point.

Solving for $\tan\theta$ from equations (4) and (5), we obtain an expression for the reflection angle function of position and offset wavenumbers $(\mathbf{k_m},\mathbf{k_h})$:

$$\tan^2\theta = \frac{(1+\gamma)^2|\mathbf{k_h}|^2 - (1-\gamma)^2|\mathbf{k_m}|^2}{(1+\gamma)^2|\mathbf{k_m}|^2 - (1-\gamma)^2|\mathbf{k_h}|^2}\,. \tag{7}$$

For the particular case of incident and reflected P waves ($\gamma = 1$), equation (7) takes the form (Sava and Fomel, 2005)

$$\tan\theta_0 = \frac{|\mathbf{k_h}|}{|\mathbf{k_m}|} \; . \tag{8}$$

Using equations (7) and (8), we can write:

$$\tan^2\theta = \frac{(1+\gamma)^2\tan^2\theta_0 - (1-\gamma)^2}{(1+\gamma)^2 - (1-\gamma)^2\tan^2\theta_0} \; . \tag{9}$$

4.2 Reflection angle δ

According to Snell's law, we can write at every image point $\frac{\sin\theta_s}{\sin\theta_r} = \gamma(\mathbf{m})$. Using the definitions of the angles made by the incident and reflected rays with the normal to the reflector and standard trigonometric identities we can write an expression that allows us to compute at every image point the angle δ function of the angle θ and the local v_p/v_s ratio:

$$\tan\delta = \frac{1-\gamma}{1+\gamma}\tan\theta \; . \tag{10}$$

Equations (7) and (10) depend both on Fourier domain quantities, $\mathbf{k_m}$ and $\mathbf{k_h}$, and on space domain quantities, $\gamma(\mathbf{m})$. This transformation can be implemented in a sequence of two transformations. In the first transformation, we can convert $\mathbf{R}(\mathbf{m},\mathbf{h})$ to $\mathbf{R}(\mathbf{m},\theta_0)$ in the Fourier domain, using equation (8). Then we can transform $\mathbf{R}(\mathbf{m},\theta_0)$ to $\mathbf{R}(\mathbf{m},\theta,\delta)$ in the space domain using equations (9) and (10).

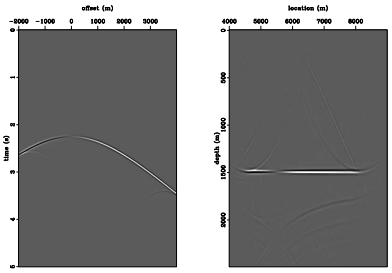

Figure 2: Synthetic data (left) and migrated image (right).

5 Example

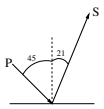

Figure 3: Simple converted-wave reflection experiment.

We illustrate the multicomponent angle-gather construction with a simple model of a flat reflector in constant velocity. The left panel of figure 2 shows one typical shot gather, and the right panel shows the image obtained by shot-record migration. The shot is located at 5500 m and the flat reflector is at 1500 m depth. The incident P-wave velocity is 2000 m/s and the reflected S-wave velocity is 1000 m/s. Given the geometry of our simple experiment, Figure 3, the incident P wave arrives at the image location at 45°, and the reflected S wave leaves the image point at approximately 21° from the normal.

Figure 4 shows one common-image gather at 4000 m. The from panel of the cube depicts the horizontal and vertical offsets, h_x and h_z respectively. For a P-P reflection, the offset vector is parallel to the reflector (horizontal in this case), therefore its vertical component $h_z = const$. This is not true for P-S reflections, even for this simple case of a flat reflector in constant media. Figure 4 illustrates that both offsets are non-zero, which invalidates the conventional common-angle constructions that are designed for P-P reflections.

Figure 4: Multi-offset converted-waves common-image gather. The vertical offset $h_z \neq const$ even for flat reflectors.

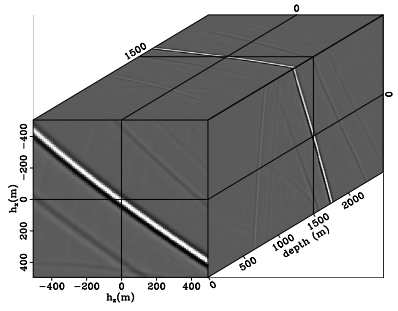

Figure 5 (middle panel) shows that conventional angle-domain mapping misplaces the reflected energy: the reflection is placed at $\tan\theta \approx 0.55$ corresponding to an incorrect reflection angle of $2\theta \approx 57°$. Figure 5 (right panel) shows the same angle-gather after converted wave correction. Now, the energy is correctly places at $\tan\theta \approx 0.65$ which corresponds to a correct reflection angle $2\theta \approx 66°$.

Figure 5: Offset-gather for a single shot (left), angle-gather constructed using the traditional P-P methodology, and angle-gather constructed using the converted methodology.

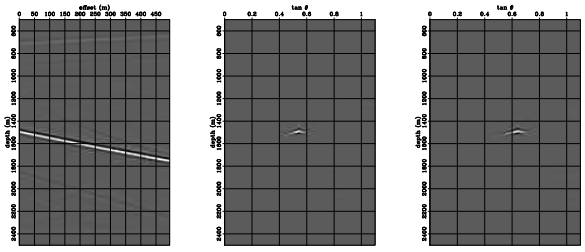

6 Conclusion

We implement angle decomposition for images constructed with shot-record migration of multicomponent data. We use full vector offsets separating sources and receivers at image points. This approach leads to a compact formulation for the incidence and reflection angles at every image points. A simple numerical experiment confirms the theory.

7 REFERENCES

Biondi, B., and Symes, W. W., 2004, Angle-domain common-image gathers for migration velocity analysis by wavefield-continuation imaging: Geophysics, **69**, 1283–1298.

de Bruin, C. G. M., Wapenaar, C. P. A., and Berkhout, A. J., 1990, Angle-dependent reflectivity by means of prestack migration: Geophysics, **55**, 1223–1234.

Gray, S. H., Etgen, J., Dellinger, J., and Whitmore, D., 2001, Seismic migration problems and solutions: Geophysics, **66**, 1622–1640.

Rickett, J. E., and Sava, P. C., 2002, Offset and angle-domain common image-point gathers for shot-profile migration: Geophysics, **67**, 883–889.

Sava, P., and Fomel, S., 2005, Coordinate-independent angle-gathers for wave equation migration *in* 75th Ann. Internat. Mtg. Soc. of Expl. Geophys.

Sava, P. C., and Fomel, S., 2003, Angle-domain common-image gathers by wavefield continuation methods: Geophysics, **68**, 1065–1074.

Stewart, R. R., Gaiser, J., Brown, R. J., and Lawton, D. C., 2002, Converted-wave seismic exploration: Methods: Geophysics, **67**, 1348–1363.

—, 2003, Converted-wave seismic exploration: Applications: Geophysics, **68**, 40–57.